Published in final edited form as:
Exp Cell Res. 2009 April 15; 315(7): 1247–1259. doi:10.1016/j.yexcr.2008.12.026.

Gravin Dynamics Regulates the Subcellular Distribution of PKA

Xiaohong Yan, **Magdalena Walkiewicz**, **Jennifer Carlson**, **Laura Leiphon**, and **Bryon Grove**
Department of Anatomy and Cell Biology, UND School of Medicine and Health Sciences, 501 N Columbia Rd., Grand Forks, ND, 58202-9037

Abstract

Gravin, a multivalent A-kinase anchoring protein (AKAP), localizes to the cell periphery in several cell types and is postulated to target PKA and other binding partners to the plasma membrane. An N-terminal myristoylation sequence and three regions rich in basic amino acids are proposed to mediate this localization. Reports indicating that phorbol ester affects the distribution of SSeCKS, the rat orthologue of gravin, further suggest that PKC may also regulate the subcellular distribution of gravin, which in turn may affect PKA distribution. In this study, quantitative confocal microscopy of cells expressing full-length and mutant gravin-EGFP constructs lacking the proposed targeting domains revealed that either the N-myristoylation site or the polybasic regions were sufficient to target gravin to the cell periphery. Moreover, phorbol ester treatment induced redistribution of gravin-EGFP from the cell periphery to a juxtanuclear vesicular compartment, but this required the presence of the N-myristoylation site. Confocal microscopy further revealed that not only did gravin-EGFP target a PKA RII-ECFP construct to the cell periphery, but PKC activation resulted in redistribution of the gravin and PKA constructs to the same subcellular site. It is postulated that this dynamic response by gravin to PKC activity may mediate PKC dependent control of PKA activity.

Introduction

It is now clear that targeting of signaling proteins and protein complexes to specific subcellular sites by scaffolding or anchoring proteins is an important mechanism for modulating intracellular signaling activities. By bringing signaling molecules in close proximity to effector proteins, these scaffolding proteins can facilitate effector protein responses and confer specificity on signaling complexes that participate in multiple signaling pathways within the cell. Localization of signaling proteins or signaling complexes to specific cellular sites also increases the complexity of signaling events that can be affected by a given number of signaling proteins.

Among the numerous scaffolding proteins that have been shown to target signaling molecules to specific subcellular sites, A-kinase anchoring proteins are perhaps the best known. More than 70 AKAPs have been described to date and they are all characterized by possessing an amphipathic helical domain which binds the regulatory subunit of PKA and a subcellular targeting domain which targets the AKAP to a specific subcellular site. AKAPs have been shown to localize to diverse subcellular locations including the plasma membrane [1,2], cytoskeleton [3], mitochondria [4,5], and nuclear envelope [6] and the functional significance

Address correspondence to: Dr. Bryon D. Grove, Department of Anatomy and Cell Biology, University of North Dakota School of Medicine and Health Sciences, 501 N. Columbia Rd. Stop 9037, Grand Forks, ND, 58202-9037.

of several of these in targeting PKA to these subcellular sites has been documented [7]. In addition to targeting PKA to subcellular sites, a number of AKAPs are multivalent and interact with several other signaling proteins including PKC, calcineurin, PP2B and PP1, and phosphodiesterases (reviewed by [7]) and likely play a role in signaling by targeting a signaling complex to specific cellular sites.

Gravin, a multivalent member of the AKAP family, was originally identified during screening of an endothelial cell expression library with serum from a patient with myasthenia gravis [8]. It was subsequently identified in a fetal brain expression library during a screen for PKA binding proteins by Nauert et al. [9] and shown to be an AKAP. Like other AKAPs, gravin has been shown to bind the PKA RII subunit in vitro [9–11] through interactions with an amphipathic helical domain near the C-terminal region between residues 1541 and 1554 [9]. Gravin has also been shown to bind PKC [9–11], β2-adrenergic receptor [12–15], PDE4D [16], Ca2+/calmodulin [17] and contains a domain that has been shown to bind cyclin D in SSeCKS, the rat orthologue of gravin [18,19]. The role of gravin in intracellular signaling events and in subsequent cellular activity is not well understood, but several reports suggest that it may be involved in a number of different cellular events. Fluorescence and electron microscopy reveal that gravin localizes to the cell periphery [10,11] suggesting that it may participate in signaling events at or near the cell membrane by targeting PKA and other signaling molecules to these sites. Consistent with this, several studies by Malbon and colleagues [12–15] indicate that gravin interacts with the β2-adrenergic receptor in A293 cells in a PKA dependent manner and plays a role in regulating β2-adrenergic receptor desensitization and resensitization. More recently, gravin has been shown to play a role in PDE4 dependent regulation of submembrane cAMP levels in HEK293 cells [16]. Gelman and colleagues on the other hand have postulated that gravin and SSeCKS may regulate cytoskeletal organization and cellular migration and play a role as a tumor suppressor. Overexpression of SSeCKS was reported to inhibit cellular migration and alter cytoskeletal organization and cell shape in several cultured cell types and to inhibit the growth of prostate tumor cells in nude mice [20–25]. Along similar lines, Weiser et al. [26] recently reported that gravin regulates cell spreading in COS7 cells. A report by Lee et al. [27] further suggests that SSeCKS expression in astrocytes may regulate endothelial permeability at the blood brain barrier.

Several lines of evidence indicate that while gravin localizes to the cell periphery, its distribution is dynamic. Several reports have shown that SSeCKS redistributes from the cell periphery to a perinuclear region in response to phorbol ester treatment. More recently, Tao et al., [17] demonstrated that elevation of intracellular calcium concentration in cells treated with A23187 resulted in redistribution of gravin from the cell periphery to the cytosol in A293 cells. This dynamic behavior of gravin in response to PKC activation and calcium flux raises the interesting possibility that gravin may redirect PKA to different subcellular sites in response to these intracellular signaling events, which in turn may interrupt specific PKA dependent signaling events at the periphery or initiate PKA dependent signaling events at other intracellular sites. If this is the case, then gravin dynamics may serve a role in mediating cross-talk between PKA dependent signaling events and either PKC or calcium mediated signaling events.

To investigate the hypothesis that gravin dynamics regulates PKA distribution, we used fluorescent protein constructs of gravin and PKA to assess subcellular targeting of PKA by gravin in response to PKC mediated changes in gravin distribution. This study revealed that PKC activation induces redistribution of gravin from the cell periphery to a juxtanuclear vesicular compartment in a manner that requires a putative N-myristoylation site. Moreover, these studies demonstrate that not only is gravin able to target PKA to the cell periphery, but that redistribution of gravin to the vesicular compartment is accompanied with redistribution of PKA to the vesicular compartment.

Materials and Methods

Construction of Gravin-EGFP and PKA-ECFP Expression Vectors

Full length and mutant gravin vector constructs lacking suspected membrane binding domains were initially constructed in pcDNA3.1-V5/His A. The full-length gravin expression vector was generated by assembling three overlapping cDNA fragments spanning the full-length gravin coding sequence between the BamHI and XbaI sites in the multiple cloning site of the vector. These fragments were generated by RT-PCR using RNA from ECV304 cells and cloned into pCR2.1 (Invitrogen, Carlsbad, CA). Mutant gravin constructs containing deletions were produced from the full length vector by replacing regions of the gravin coding sequence with either short linker sequences or with PCR generated cDNA fragments that contained deletions in the sequence. The residues deleted in the mutant vectors are indicated in Fig. 1.

Full length and mutant gravin-EGFP constructs lacking the suspected membrane binding domains were made by first inserting the full length gravin sequence into pEGFP-N2 (Clontech Labs, Inc., Mountain View, CA) between the EcoRI site and an XbaI site that had been added to the original pEGFP-N2 vector and then replacing the 5' half of the gravin sequence in the gravin-EGFP construct between the EcoRI and EcoRV restriction enzyme sites with the corresponding mutant regions from the mutant gravin constructs described above.

A mutant gravin-EGFP construct lacking the C-terminal 861 amino acids (which includes the PKA binding domain) was generated by replacing a 2609 base fragment between the EcoR V and Xma I sites in the full length sequence with a 23 bp linker sequence (5'ATCTGCTTCAGTGACAGAACCTC3'). A PKA RII-ECFP construct was generated by inserting a PCR generated cDNA corresponding to the human PKA RII β sequence into the KpnI and Bst BI sites of a modified pcDNA3.1 vector. A PCR generated ECFP cDNA sequence was then inserted in frame with the PKA RII sequence to produce a construct in which ECFP was fused to the C-terminus of PKA RIIβ via an intervening 11 residue linker (FEYPYDVPDYA).

Cell culture and Transfection

AN3 CA cells and HEC-1-A cells were obtained from the American Type Culture Collection (Manassas, VA, ATCC numbers: HTB-111, HTB-112 respectively). AN3 CA cells, which are derived from a metastatic lesion in the lymph node of a patient with endometrial carcinoma, do not express gravin. HEC-1-A cells, another endometrial carcinoma cell line, express gravin sporadically in clusters of cells. The cell lines were cultured in Dulbecco's Modified Eagle's Medium (DMEM) with 10% fetal bovine serum and 100 units/ml penicillin and 100 μg/ml streptomycin in a 37 °C incubator with 5% CO_2 atmosphere. The media were replaced by fresh growth media three times a week and cells were split 1:20 once a week when they reached confluence.

In all experiments involving transfection of cells with expression vectors, cells were transfected three days after seeding. To perform a transfection, cells were incubated with OPTI-MEM I (Gibco/Invitrogen) transfection solution containing 1μg/ml plasmid and 10μl/ml Lipofectamine (Invitrogen) at 37 °C for 5 hours. Following incubation, cells were washed with OPTI-MEM I, which was then replaced with DMEM growth media. Twenty-four hours and forty-eight hours later, cells were processed for microscopy or Western blot analysis respectively.

Western blotting

To obtain protein samples for Western Blotting, transfected AN3 CA cells in T-25 flasks were harvested by scraping into 1 ml of ice-cold PBS (58 mM Na_2HPO_4, 17 mM NaH_2PO_4-H_2O,

68 mM NaCl), pelleted by centrifugation, and homogenized in 100 μl of lysis buffer [20 mM Tris base, 150 mM NaCl, 10 mM EDTA, 10 mM Benzamidine HCl, 1% (v/v) Triton X-100, 0.05% (v/v), Tween 20, 1 mM PMSF and 100 μg/ml leupeptin] by brief sonication. Cell homogenates were then run on a 5% SDS-polyacrylamide gel and transferred to nitrocellulose membranes by standard methods [28]. Blots were probed using an anti-gravin polyclonal antibody [10,29] and immunoreactive bands were detected by chemiluminescence.

Immunofluorescence and confocal microscopy

For immunofluorescence microscopy studies, cells seeded onto either 12 mm or 25 mm diameter coverslips (Fisher Scientific, Pittsburgh, PA) were fixed with 3.7% paraformaldehyde in PBS, rinsed with PBS, permeabilized with digitonin, treated with 5% normal goat serum to block non-specific binding of the antibody, and then treated with an anti-gravin monoclonal antibody. Primary antibody labeling was then detected using a Cy3 conjugated donkey anti-mouse secondary antibody (Jackson Immunoresearch, Inc., West Grove, PA). Labelled cells were imaged using either an Olympus Fluoview 300 confocal microscope or a Zeiss 510 META confocal microscope.

For imaging of live cells, cells seeded onto either 12 mm or 25 mm diameter coverslips (Bellco Glass, Vineland, NJ; Fisher Scientific) and transfected with the gravin-EGFP constructs and the PKA RII ECFP construct were placed into an Attofluor imaging chamber (Molecular Probes/Invitrogen) and imaged using the Olympus Fluoview 300 and Zeiss 510 META confocal microscopes. In cases where imaging was performed over several minutes, cells were incubated in Leibovitz's L-15 media (Gibco/Invitrogen) and maintained at 37°C using a heating stage.

Due to the fact that the EGFP and ECFP spectra overlap, two color imaging of cells co-transfected with EGFP and ECFP constructs was performed using the Zeiss Meta detector and linear unmixing. Pilot experiments were performed beforehand to determine the appropriate number and range of spectral channels required to avoid channel cross-over. Based on these pilot experiments, samples were excited at 458 nm (50% laser power) and images were collected in three spectral channels covering an emission detection range of 463.2 to 559.5 nm. Reference spectra were obtained from images of cells expressing either PKA RII-ECFP alone or one of the gravin-EGFP constructs alone. Linear unmixing was performed using the linear unmixing algorithm provided in the Zeiss operating software (Version 3.2 SP2).

Image analysis

To assess the role of the putative myristoylation site and the three polybasic regions in targeting gravin to the cell periphery, AN3 CA cells cultured on 12 mm glass coverslips were transfected with either the full-length gravin-EGFP vector, the mutant gravin-EGFP vector constructs, or EGFP alone. Forty-eight hours following transfection, the transfected cells were incubated with 16 μM FM4-64 at 37 °C for 30 minutes to label the plasma membrane and then images of the cells were collected for quantitative analysis of gravin-EGFP distribution using an Olympus Fluoview 300 confocal microscope.

For each field of view, a multichannel image was collected with one channel corresponding to the EGFP fluorescence, one channel corresponding to the FM4-64 fluorescence and a third channel corresponding to the differential interference phase contrast (DIC) image of the cells in the field (Fig. 2A, 2B, 2C). Each of the three images were collected sequentially using a 488 nm laser line and a 510–540 nm band pass emission filter (FVX-BA510–540) to detect the EGFP signal, a 543 nm laser line and a 565 nm long pass emission filter (FVA-BA565IF) to detect FM4-64 signal, and transmitted light from the 488 nm laser line to obtain DIC image.

The same acquisition parameters (laser intensity=50%, photomultiplier tube voltage=700, amplifier gain=1 and offset=0%) were used throughout the entire data collection process.

To the quantify the relative proportion of EGFP fluorescence at the cell periphery, the images were first converted to grayscale images (Fig. 2D, E, F) and then regions of interest for the plasma membrane, the entire cell and the nucleus were defined using ImageJ 1.29x software. The region of interest corresponding to the plasma membrane was defined by processing the grayscale FM4-64 image (Fig. 2D) through a Hessian filter plug-in for ImageJ (Feature J written by Erik Meijering, Biomedical Imaging Group Rotterdam of the Erasmus MC - University Medical Center Rotterdam, Netherlands) and then adjusting the threshold of the resulting images (Fig. 2G and 2H) to produce an image (Fig. 2I) from which a highlighted region corresponding to the FM4-64 labeled plasma membrane could be extracted (2J). The region of interest corresponding to the entire cell was generated by highlighting the interior area enclosed within the highlighted membrane regions (Fig. 2L). The region of interest corresponding to the nucleus in each cell was defined by highlighting the nuclear region in the DIC image by hand (Fig. 2K). These regions were then superimposed on the EGFP images (Fig. 2M, N, O) and the average EGFP fluoresence within the regions was determined. Background fluorescence was determined by measuring the fluorescence intensity in regions of interest in cells in the same field that were not expressing the gravin-EGFP transgene product. The fluoresence intensity measurements were then used to calculate the ratio of the mean fluorescence intensity in the plasma membrane region versus the mean fluorescence intensity in the cell (cytoplasm plus plasma membrane) for each of the transfectants using the following formula:

$$R_{mem/cell} = \frac{F_{membrane} - F_{background(membrane)}}{F_{cell} - F_{background(cell)}}$$

where $F_{membrane}$ represented the mean fluorescence intensity at the plasma membrane measured from images of cells expressing the gravin-EGFP transgene product, $F_{background(membrane)}$ and $F_{background(cell)}$ represented the background fluorescence intensity measured from images of cells not expressing the gravin-EGFP transgene product, and F_{cell} represented the mean fluorescence intensity of the cell (cytoplasm plus plasma membrane). Because the gravin-EGFP fusion protein was always excluded from the nuclear region, F_{cell} was calculated by the following formula:

$$F_{cell} = \frac{F_{total} \times S_{total} - F_{nucleus} \times S_{nucleus}}{S_{total} - S_{nucleus}}$$

where F_{total} and $F_{nucleus}$ refer to the mean fluorescence intensities of the entire cell and of the nucleus respectively and S_{total} and $S_{nucleus}$ refer to the areas of the entire cell and of the nucleus respectively.

The samples were collected from 39 to 94 AN3 CA cells from each gravin-EGFP vector transfection, which were repeated at least twice. Full-length gravin-EGFP and EGFP-N2 transfectants were included in each repeat as standards. One-way ANOVA tests showed that ratios calculated from the same transfectant from different repetitions were not significantly different from each other and therefore the ratios from all transfectants transfected with the same construct were pooled together. The mean difference among the transfectants was analyzed by One-way ANOVA test using SPSS student version 10 using a p value for significance of $P < .01$. Scheffe Post Hoc tests with $\alpha = .01$ were used to compare the distribution of each gravin-EGFP vector against the distribution of other gravin-EGFP vectors. An

homogeneous subset analysis was also performed to assess the similarity among these gravin-EGFP fusion proteins.

Results

Subcellular Distribution of Gravin

To study the subcellular distribution of gravin, two endometrial adenocarcinomal cell lines, HEC-1-A cells and AN3 CA cells were used. HEC-1-A cells immunolabeled with an anti-gravin antibody showed that endogenous gravin was expressed sporadically in clusters of cells. In those cells expressing gravin, gravin localized to the cell periphery, especially to cell-cell contacts (Fig. 3A). In contrast, expression of gravin could not be detected in AN3 CA cells using the same immunolabeling approach as that for labeling HEC-1-A cells (Fig. 3B). However, in AN3 CA cells transfected with the gravin-V5/His vector, immunofluorescence microscopy revealed that the gravin-V5/His fusion protein was expressed at the cell periphery, similar to the endogenous gravin in HEC-1-A cells (Fig. 3C). Full-length gravin-EGFP also localized at the cell periphery in live transiently transfected AN3 CA cells (data not shown).

Treatment of cells with PMA induced a dramatic change in the distribution of gravin. Immunofluorescence microscopy of HEC-1-A cells after PMA treatment revealed complete loss of peripheral labeling within 30 minutes treatment and an accumulation of labeling in a juxtanuclear region (Fig. 4). The distribution of gravin immunofluorescence did not change in cells treated with PMA in the presence of bis-indolylmaleimide, a general PKC inhibitor. Gravin-EGFP also changed distribution after PMA treatment in HEC-1-A and AN3 CA cells transfected with a full length gravin-EGFP construct. Gravin-EGFP disappeared from the membrane within 10 minutes following PMA treatment and reached its highest levels of concentration in the juxtanuclear region within 30 minutes (Fig. 5). Confocal microscopy revealed that the juxtanuclear gravin-EGFP was associated with concentration of gravin-EGFP at the rims of small juxtanuclear vesicles.

Identification of Domains Responsible for Plasma Membrane Binding

A putative N-terminal myristoylation site and three domains rich in basic amino acids at residues 171–191, 296–316 and 507–536 respectively are present in gravin. To address the question whether these domains target gravin to the plasma membrane, a series of gravin-EGFP vectors encoding gravin-EGFP constructs lacking these hypothesized membrane binding domains were generated by molecular cloning approaches (Fig. 1).

The expression of the different gravin-EGFP vectors in AN3 CA cells was confirmed by detecting the fusion proteins by Western Blot using an anti-gravin antibody, which recognizes an epitope close to the C-terminus of gravin. This antibody also detected endogenous gravin in ECV cells but did not detect gravin in control untransfected AN3 CA cells. In the lanes loaded with lysates from different gravin-EGFP transfectants, expression of gravin was detected and the position of gravin bands matched the size of the desired gravin-EGFP mutants (Fig. 6).

Confocal microscopy of AN3 CA cells transfected with the full-length gravin-EGFP vectors, its mutants and pEGFP-N2 revealed three patterns of distribution. Δmyr, the mutant gravin-EGFP lacking the N-terminal 78 amino acids, and ΔPB1,2,3, the mutant gravin-EGFP lacking residues 42–554 showed peripheral localization, very similar to the distribution of the full-length gravin-EGFP (Fig. 7A, 7B, 7C). In cells expressing Δmyr+PB2,3, the mutant gravin-EGFP containing the first polybasic region (Fig. 7D), Δmyr+PB1,3, the mutant gravin-EGFP containing the second polybasic region (Fig. 7E), or Δmyr+PB1,2, the mutant gravin-EGFP containing the third polybasic region (Fig. 7F), fusion proteins partially localized to the cell

periphery, especially at the cell-cell contact sites, but not all the way along the cell margin. More dramatically, Δmyr+PB1,2,3, the mutant gravin-EGFP lacking the N-terminal 5 amino acids and the fragment containing all three polybasic regions (Fig. 7G), and Δ1–706, the mutant gravin-EGFP lacking the N-terminal 706 amino acids (Fig. 7H), did not localize to the cell periphery, but instead were diffusely distributed throughout the cytoplasm in a manner similar to that seen for EGFP alone, with the exception that the fusion proteins were excluded from the nuclei (Fig. 7I).

Quantitative analysis of the proportion of the EGFP fluorescence at the cell periphery relative to the EGFP fluorescence across the cell in AN3 CA cells transfected with the full-length gravin-EGFP vector and its mutant vectors further confirmed that deletion of the putative N-myristoylation site and the polybasic domains affected gravin-EGFP distribution (Fig. 8). One way ANOVA and a Scheffe post-hoc test revealed that the relative level of fluorescence at the cell periphery for the full-length gravin construct, the gravin constructs lacking either the myristoylation site or the three polybasic regions and the gravin constructs lacking the myristoylation site and any two polybasic domains was significantly greater than ($p<0.01$) that of gravin constructs lacking both the myristoylation site and all three polybasic domains or of EGFP alone. Moreover, statistical analysis (Scheffe post-hoc test) revealed three distinct localization categories for the constructs tested: a subset displaying a high level of peripheral localization which included full-length gravin, Δ-myr gravin and Δ−PB1,2,3 gravin, a subset consisting of the Δmyr+PB2,3, Δmyr+PB1,3 and Δmyr+PB1,2 constructs which displayed a moderate level of peripheral localization, and a third subset displaying the least amount of peripheral localization which included the Δmyr+PB1,2,3 and Δ1–706 gravin constructs and EGFP alone.

Role of membrane targeting domains in dynamic redistribution of gravin

To assess the role of the putative N-myristoylation site and the polybasic domains in targeting of gravin to the intracellular compartment after PKC activation, HEC-1-A cells transfected with full length gravin–EGFP, mutant gravin-EGFP lacking the putative myristoylation site (Δmyr), mutant gravin-EGFP lacking the polybasic regions, (ΔPB1,2,3), and mutant gravin-EGFP lacking both the myristoylation and polybasic domains (Δmyr+PB1,2,3) were treated with PMA. Confocal microscopy revealed that full length gravin-EGFP and ΔPB1,2,3 gravin-EGFP both disappeared from the cell periphery after PMA treatment and appeared on small vesicles concentrated in the juxtanuclear region of the cell (Fig. 9A, B, E, F). In cells transfected with the Δmyr construct, however, Δmyr gravin-EGFP disappeared from the cell periphery, but remained in the cytosol and did not concentrate on juxtanuclear vesicles (Fig. 9C, G). The Δmyr+PB1,2,3 construct was cytosolic and did not change distribution after PMA treatment (Fig. 9D, H).

Role of gravin in targeting PKA

The role of gravin in targeting PKA to subcellular sites was investigated by testing the effect of expressing gravin-EGFP constructs in HEC-1-A and AN3 CA cells on PKA-ECFP distribution in these cells. Because confocal imaging in these experiments required the use of a spectral detector and post acquisition image processing (linear unmixing) to separate the individual fluorescent protein signals, some constraints were placed on the level of construct expression required for the ECFP and EGFP signals to be resolved and limited the degree to which transfected cultures could be evaluated statistically. In spite of this, it was possible to identify cells in which the subcellular distribution of the ECFP and EGFP constructs could be resolved.

In cells transfected with the PKA RII-ECFP vector alone, PKA RII-ECFP was diffusely distributed throughout the cytoplasm, but was excluded from the nuclei. No specific region

displayed a concentration of PKA RII-ECFP (Fig. 10A, F and K, P). However, in most cotransfected cells in which full-length gravin-EGFP and PKA RII-ECFP could be easily distinguished, PKA RII-ECFP was concentrated at the cell periphery, overlapping with the full-length gravin-EGFP at the cell periphery (Fig. 10C, H and M, R). In the control cells transfected with full-length gravin-EGFP alone, little signal from EGFP crossed over to the ECFP channel after linear unmixing (Fig. 10G, Q). PKA RII-ECFP showed a different pattern of distribution in cells coexpressing mutant gravin-EGFP fusion proteins. In cells cotransfected with Δmyr+PB1,2,3 gravin-EGFP and PKA RII-ECFP vectors, both Δmyr+PB1,2,3 gravin-EGFP and PKA RII-ECFP were diffusely distributed throughout the cytoplasm (Fig. 10D, I and N, S). In cells cotransfected with Δ-PKA gravin-EGFP and PKA RII-ECFP vectors, the gravin fusion protein localized at the cell periphery (Fig. 10E, O), but PKA RII-ECFP was diffusely distributed throughout the cytoplasm (Fig. 10J, T).

To determine if PKA changed its distribution in response to PMA in the presence of gravin, HEC-1-A and AN3 CA cells were transfected with PKA RII-ECFP vector alone, cotransfected with PKA RII-ECFP and the full-length gravin-ECFP vectors, or cotransfected with PKA RII-ECFP and Δ-PKA gravin-EGFP vectors. In cells expressing only PKA RII-ECFP, the PKA RII fusion protein did not change distribution in response to PMA treatment and remained diffusely distributed throughout the cytoplasm (Fig. 11A, F and K, P). In contrast, in most cells where coexpressed full-length gravin-EGFP and PKA RII-ECFP could be easily distinguished in images, both constructs redistributed to the juxtanuclear compartment after PMA treatment and PKA RII-ECFP colocalized with the full-length gravin-EGFP at vesicle membranes (Fig. 11B, G, C, H and L, Q, M, R). However, in cells expressing Δ-PKA gravin, the mutant gravin-EGFP lacking a region containing the PKA binding domain, the mutant gravin translocated to the juxtanuclear region after PMA treatment (Fig. 11D, E and N, O), but PKA RII-ECFP remained diffusely distributed throughout the cytoplasm with reduced ECFP fluorescence in the region where the mutant gravin-EGFP was concentrated (Fig. 11I, J and S, T).

Discussion

The goal of the current study was to evaluate domains responsible for targeting gravin to the cell periphery and other compartments and to demonstrate that dynamic relocalization of gravin can regulate PKA distribution. The current study demonstrates that targeting of gravin to the cell periphery is mediated by both a putative N-terminal myristoylation site and three polybasic domains. This study also reveals that gravin is a dynamic protein that undergoes redistribution to an intracellular vesicular compartment in response to PKC activation and that the putative N-terminal myristoylation is required for this redistribution. Finally, changes in gravin distribution alters targeting of PKA to different subcellular sites.

The current study is the first to report that gravin undergoes redistribution from the cell periphery to a juxtanuclear vesicular compartment in response to activation of PKC by phorbol ester. Previously, Piontek and Brandt [11] reported that PKC activation resulted in redistribution of gravin from the plasma membrane to a cytosolic fraction in NT-2 cells. However, the possibility that gravin may associate with an intracellular membranous compartment was not explored. Gelman and colleagues [21,30] reported several times that SSeCKS, the rat orthologue of gravin, underwent redistribution from the cell periphery to a perinuclear location in several cultured cell types after phorbol ester treatment, but these studies did not determine if this compartment was cytosolic or vesicular in nature. In a study of SSeCKS/β-galactosyltransferase interactions, Wassler et al., [31] also reported that SSeCKS localized to a juxtanuclear region after phorbol ester treatment and postulated that SSeCKS may associate with the Golgi apparatus due to its proposed association with β-galactosyltransferase, but this was not confirmed and awaits further investigation. More recently, Streb et al., [32] reported that full-length SSeCKS constructs in transfected in COS7

cells localized to the endoplasmic reticulum, but these cells were not treated with phorbol ester and therefore this distribution differs from that reported by other investigators. In the current study, gravin strongly localized to the cell periphery until cells were treated with phorbol ester after which gravin accumulated around the periphery of intracellular vesicles. Further investigations to identify the vesicular compartment to which gravin trafficks in response to PMA treatment will be critically important to fully understanding the importance of gravin dynamics in regulating intracellular signalling.

Deletion experiments in this study clearly demonstrated that two domains in the N-terminal half of gravin play different roles in the dynamic targeting of gravin to peripheral and intracellular compartments. Image analysis showed that either a putative N-myristoylation site or three polybasic regions were sufficient to target gravin to the cell periphery. In fact, the presence of any single polybasic region in gravin constructs was sufficient to target gravin to the cell periphery all be it to a lesser extent. However, the putative N-myristoylation site was required for targeting of gravin to the juxtanuclear vesicular compartment. Constructs lacking the N-myristoylation site, but containing the polybasic domains dissociated from the cell periphery in response to phorbol ester treatment, but remained cytosolic in their distribution and did not localize with a juxtanuclear vesicular compartment.

The finding in this study that the N-myristoylation site and three polybasic domains play a role in targeting gravin to the cell periphery is consistent with studies of membrane targeting domains in other proteins. AKAP79, which does not possess an N-myristoylation site, has been shown to be targeted to the plasma membrane by three polybasic domains comparable in organization to those in gravin and deletion studies demonstrated that any two of the polybasic regions were sufficient to target AKAP79 to the cell periphery [2]. Similarly, a polybasic domain termed the effector domain in MARCKS, a protein implicated in diverse functions including neurosecretion, actin filament organization, cellular migration, and phagocytosis, has been shown to play an essential role in MARCKS-plasma membrane interactions [33–36]. Our observation that the polybasic domains in gravin constructs were sufficient to target gravin to the cell periphery is consistent with reports by Tao et al. [17] and others [36]. In their study, Tao et al [17] demonstrated that the polybasic domains were sufficient for targeting gravin to the cell periphery, likely through interactions with membrane phospholipids, and showed that the presence of any two polybasic domains in constructs lacking the myristoylation site was necessary for gravin to regulate β2-adrenergic receptor resensitization. This study, however, did not investigate the role of N-myristoylation in gravin-membrane interactions. N-terminal myristoylation has been shown play a role in protein-plasma membrane binding in a number of proteins [37], and although a second signal, either in the form of palmitoylation or the presence of regions rich in basic amino acids, has been shown to be required in some instances [reviewed by 38,39], N-myristoylation alone has been shown to be sufficient for membrane targeting in some proteins (e.g. NCS-1 and hippocalcin) [40–44]. This appears to be the case for gravin in the present study. Deletion of the polybasic domains resulted in no observable decrease in membrane localization of the gravin-EGFP construct compared to the full-length gravin construct. Constructs used by Tao et al. [17] to investigate the role of the polybasic domains in β2-adrenergic receptor activity lacked the N-myristoylation site. Thus it remains to be determined if gravin targeted to the plasma membrane by N-myristoylation alone may also regulate β2-adrenergic receptor. However, the fact that the myristoylation site alone targets gravin to the membrane and is required for targeting to intracellular compartments indicates that N-myristoylation of gravin is important in gravin-membrane interactions and in regulating gravin dynamics.

The mechanism underlying PKC mediated translocation of gravin has yet to be fully elucidated. Phosphorylation of the polybasic regions in gravin has been proposed to regulate plasma membrane-gravin interactions in much the same way that PKC dependent phopshorylation has

been shown to alter the binding of MARCKS to the plasma membrane [17,36]. Several lines of evidence, including in vitro phosphorylation studies [30] and site directed mutagenesis of putative phosphorylation sites in the membrane binding domain [45], support this hypothesis. However, the behavior of constructs in the current study indicate that PKC-mediated gravin translocation may be more complex than this. Mutant gravin lacking the polybasic domains and the putative PKC binding domain [9] underwent the same PKC-mediated change in distribution that was observed for wild-type gravin. All predicted PKC phosphorylation sites found in the membrane binding domains were lacking in this construct and thus while gravin-membrane interactions may be regulated by phosphorylation of these domains, other PKC dependent mechanisms must play a role as well. It is possible that PKC-mediated phosphorylation of other regions of this construct could have effected its association with the plasma membrane and may play a role in PMA induced translocation of gravin to a cytosolic compartment. Alternatively, phosphorylation of either membrane or cortical proteins may alter gravin-membrane interactions thereby resulting in loss of plasma membrane binding and translocation to an cytosolic or vesicular compartment. Further work is required to fully understand the mechanism underlying PKC mediated gravin redistribution to the vesicular compartment.

The finding that PKA RII underwent redistribution in a gravin-dependent fashion in response to PKC activation supports the hypothesis that changes in gravin distribution may regulate PKA dependent signaling within different subcellular compartments. Previously, studies by Nauert et al. [9] and others [10] demonstrated using coimmunoprecipitation and overlay approaches that gravin bound to the regulatory subunit of PKA. More recently, Piontek and Brandt [11] demonstrated using subcellular fractionation and immunoprecipitation approaches that gravin-PKA RII complexes not only localized to a plasma membrane fraction, but underwent redistribution from the plasma membrane fraction to a cytosolic fraction after PKC activation. Experiments in the current study showing that gravin targeted PKA RII to the cell periphery in cotransfected cells and that redistribution of gravin to an intracellular vesicular compartment resulted in redistribution of PKA RII to the same compartment confirm and add to these previous studies by providing direct in vivo evidence that gravin is able to target PKA to subcellular compartments in a dynamic manner. From all of these results, it is postulated that PKC mediated gravin dynamics may serve as a mechanism for cross-talk between different signaling pathways – in this case, between PKC and PKA. By altering PKA RII localization at the plasma membrane, gravin dynamics in response to PKC activation may serve as a switch that turns PKA signaling events off at the cell periphery as gravin dissociates from the plasma membrane. At the same time, localization of a gravin-PKA complex to an intracellular vesicular compartment may engage a PKA-dependent signaling event or events at this new compartment. Because the identity of the intracellular vesicular compartment is currently unknown, the significance of PKA localization to this compartment is unclear. Thus, the identification of this compartment may be critical to fully understanding the importance of gravin dynamics in intracellular signaling. If changes in gravin distribution do effect PKA dependent signaling events, then other intracellular signaling events that effect gravin distribution may affect PKA signaling as well. Tao et al. [17] recently demonstrated that elevated intracellular calcium induces redistribution of gravin from the plasma membrane to the cytosol through interactions between gravin and calcium-calmodulin. Although it is unknown to what degree gravin-PKA interactions might also be effected by elevated intracellular calcium, it is reasonable to speculate that calcium-calmodulin mediated loss of gravin-plasma membrane binding would alter PKA signaling at the plasma membrane. Along similar lines, other gravin binding partners such as PDE4 [16] may also be redirected to new locations by changes in gravin distribution and participate in new or different signaling events. It is clear from these studies that further investigation of gravin dynamics will likely lead to new insights into the role of this scaffolding protein in regulating intracellular signaling.

Acknowledgments

This work was supported in part by seed funds from the University of North Dakota. Imaging studies were conducted in the UNDSMHS Basic Sciences Imaging Center which is supported in part by funds awarded through a COBRE grant (NIH 2 P20 RR07699-06). We thank Dr. Patrick Carr for reading the manuscript and providing valuable comments.

References

1. Fraser ID, Tavalin SJ, Lester LB, Langeberg LK, Westphal AM, Dean RA, Marrion NV, Scott JD. A novel lipid-anchored A-kinase Anchoring Protein facilitates cAMP-responsive membrane events. EMBO J 1998;17:2261–2272. [PubMed: 9545239]
2. Dell'Acqua ML, Faux MC, Thorburn J, Thorburn A, Scott JD. Membrane-targeting sequences on AKAP79 bind phosphatidylinositol-4, 5-bisphosphate. Embo J 1998;17:2246–2260. [PubMed: 9545238]
3. Westphal RS, Soderling SH, Alto NM, Langeberg LK, Scott JD. Scar/WAVE-1, a Wiskott-Aldrich syndrome protein, assembles an actin-associated multi-kinase scaffold. EMBO J 2000;19:4589–4600. [PubMed: 10970852]
4. Affaitati A, Cardone L, de Cristofaro T, Carlucci A, Ginsberg MD, Varrone S, Gottesman ME, Avvedimento EV, Feliciello A. Essential role of A-kinase anchor protein 121 for cAMP signaling to mitochondria. J Biol Chem 2003;278:4286–4294. [PubMed: 12427737]
5. Cardone L, de Cristofaro T, Affaitati A, Garbi C, Ginsberg MD, Saviano M, Varrone S, Rubin CS, Gottesman ME, Avvedimento EV, Feliciello A. A-kinase anchor protein 84/121 are targeted to mitochondria and mitotic spindles by overlapping aminoterminal motifs. J Mol Biol 2002;320:663–675. [PubMed: 12096916]
6. Kapiloff MS, Schillace RV, Westphal AM, Scott JD. mAKAP: an A-kinase anchoring protein targeted to the nuclear membrane of differentiated myocytes. J Cell Sci 1999;112(Pt 16):2725–2736. [PubMed: 10413680]
7. Wong W, Scott JD. AKAP signalling complexes: focal points in space and time. Nat Rev Mol Cell Biol 2004;5:959–970. [PubMed: 15573134]
8. Gordon T, Grove B, Loftus JC, O'Toole T, McMillan R, Lindstrom J, Ginsberg MH. Molecular cloning and preliminary characterization of a novel cytoplasmic antigen recognized by myasthenia gravis sera. J Clin Invest 1992;90:992–999. [PubMed: 1522245]
9. Nauert JB, Klauck TM, Langeberg LK, Scott JD. Gravin, an autoantigen recognized by serum from myasthenia gravis patients, is a kinase scaffold protein. Curr Biol 1997;7:52–62. [PubMed: 9000000]
10. Grove BD, Bruchey AK. Intracellular distribution of gravin, a PKA and PKC binding protein, in vascular endothelial cells. J Vasc Res 2001;38:163–175. [PubMed: 11316952]
11. Piontek J, Brandt R. Differential and regulated binding of cAMP-dependent protein kinase and protein kinase C isoenzymes to gravin in human model neurons: Evidence that gravin provides a dynamic platform for the localization for kinases during neuronal development. J Biol Chem 2003;278:38970–38979. [PubMed: 12857743]
12. Fan G, Shumay E, Wang H, Malbon CC. The scaffold protein gravin (cAMP-dependent protein kinase-anchoring protein 250) binds the beta 2-adrenergic receptor via the receptor cytoplasmic Arg-329 to Leu-413 domain and provides a mobile scaffold during desensitization. J Biol Chem 2001;276:24005–24014. [PubMed: 11309381]
13. Lin F, Wang H, Malbon CC. Gravin-mediated formation of signaling complexes in β_2-adrenergic receptor desensitization and resensitization. J. Biol. Chem 2000;275:19025–19034. [PubMed: 10858453]
14. Shih M, Lin F, Scott JD, Wang HY, Malbon CC. Dynamic complexes of β2-adrenergic receptors with protein kinases and phosphatases and the role of gravin. J. Biol. Chem 1999;274:1588–1595. [PubMed: 9880537]
15. Tao J, Wang HY, Malbon CC. Protein kinase A regulates AKAP250 (gravin) scaffold binding to the beta2-adrenergic receptor. Embo J 2003;22:6419–6429. [PubMed: 14657015]
16. Willoughby D, Wong W, Schaack J, Scott JD, Cooper DM. An anchored PKA and PDE4 complex regulates subplasmalemmal cAMP dynamics. Embo J 2006;25:2051–2061. [PubMed: 16642035]

17. Tao J, Shumay E, McLaughlin S, Wang HY, Malbon CC. Regulation of AKAP-membrane interactions by calcium. J Biol Chem 2006;281:23932–23944. [PubMed: 16762919]
18. Lin X, Gelman IH. Calmodulin and cyclin D anchoring sites on the Src-suppressed C kinase substrate, SSeCKS. Biochem Biophys Res Commun 2002;290:1368–1375. [PubMed: 11820772]
19. Lin X, Nelson P, Gelman IH. SSeCKS, a major protein kinase C substrate with tumor suppressor activity, regulates G1→S progression by controlling the expression and cellular compartmentalization of cyclin D. Mol Cell Biol 2000;20:7259–7272. [PubMed: 10982843]
20. Gelman IH. The role of SSeCKS/gravin/AKAP12 scaffolding proteins in the spaciotemporal control of signaling pathways in oncogenesis and development. Front Biosci 2002;7:d1782–d1797. [PubMed: 12133808]
21. Gelman IH, Lee K, Tombler E, Gordon R, Lin X. Control of cytoskeletal architecture by the src-suppressed C kinase substrate, SSeCKS. Cell Motil Cytoskeleton 1998;41:1–17. [PubMed: 9744295]
22. Gelman IH, Tombler E, Vargas J Jr. A role for SSeCKS, a major protein kinase C substrate with tumour suppressor activity, in cytoskeletal architecture, formation of migratory processes, and cell migration during embryogenesis. Histochem J 2000;32:13–26. [PubMed: 10805381]
23. Nelson PJ, Moissoglu K, Vargas J Jr, Klotman PE, Gelman IH. Involvement of the protein kinase C substrate, SSeCKS, in the actin-based stellate morphology of mesangial cells. J Cell Sci 1999;112:361–370. [PubMed: 9885289]
24. Su B, Zheng Q, Vaughan MM, Bu Y, Gelman IH. SSeCKS metastasis-suppressing activity in MatLyLu prostate cancer cells correlates with vascular endothelial growth factor inhibition. Cancer Res 2006;66:5599–5607. [PubMed: 16740695]
25. Xia W, Unger P, Miller L, Nelson J, Gelman IH. The Src-suppressed C kinase substrate, SSeCKS, is a potential metastasis inhibitor in prostate cancer. Cancer Res 2001;61:5644–5651. [PubMed: 11454719]
26. Weiser DC, Julien KR, Lang JS, Kimelman D. Cell shape regulation by Gravin requires N-terminal membrane effector domains. Biochem Biophys Res Commun. 2008
27. Lee SW, Kim WJ, Choi YK, Song HS, Son MJ, Gelman IH, Kim YJ, Kim KW. SSeCKS regulates angiogenesis and tight junction formation in blood-brain barrier. Nat Med 2003;9:900–906. [PubMed: 12808449]
28. Towbin H, Staehelin T, Gordon J. Electrophoretic transfer of proteins from polyacrylamide gels to nitrocellulose sheets; procedure and some applications. Proc. Natl. Acad. Sci., U.S.A 1979;76:4350–4354. [PubMed: 388439]
29. Grove B, Bowditch R, Gordon T, del Zoppo G, Ginsberg M. Restricted endothelial cell expression of gravin *in vivo*. Anat. Rec 1994;239:231–242. [PubMed: 7943755]
30. Lin X, Tombler E, Nelson PJ, Ross M, Gelman IH. A novel src- and ras-suppressed protein kinase C substrate associated with cytoskeletal architecture. J Biol Chem 1996;271:28430–28438. [PubMed: 8910468]
31. Wassler MJ, Foote CI, Gelman IH, Shur BD. Functional interaction between the SSeCKS scaffolding protein and the cytoplasmic domain of beta1,4-galactosyltransferase. J Cell Sci 2001;114:2291–2300. [PubMed: 11493668]
32. Streb JW, Kitchen CM, Gelman IH, Miano JM. Multiple promoters direct expression of three AKAP12 isoforms with distinct subcellular and tissue distribution profiles. J Biol Chem 2004;279:56014–56023. [PubMed: 15496411]
33. Arbuzova A, Schmitz AA, Vergeres G. Cross-talk unfolded: MARCKS proteins. Biochem J 2002;362:1–12. [PubMed: 11829734]
34. Gambhir A, Hangyas-Mihalyne G, Zaitseva I, Cafiso DS, Wang J, Murray D, Pentyala SN, Smith SO, McLaughlin S. Electrostatic sequestration of PIP2 on phospholipid membranes by basic/aromatic regions of proteins. Biophys J 2004;86:2188–2207. [PubMed: 15041659]
35. McLaughlin S, Aderem A. The myristoyl-electrostatic switch: a modulator of reversible protein-membrane interactions. Trends Biochem Sci 1995;20:272–276. [PubMed: 7667880]
36. Seykora JT, Myat MM, Allen LA, Ravetch JV, Aderem A. Molecular determinants of the myristoyl-electrostatic switch of MARCKS. J Biol Chem 1996;271:18797–18802. [PubMed: 8702537]
37. Selvakumar P, Lakshmikuttyamma A, Shrivastav A, Das SB, Dimmock JR, Sharma RK. Potential role of N-myristoyltransferase in cancer. Prog Lipid Res 2007;46:1–36. [PubMed: 16846646]

38. Resh MD. Fatty acylation of proteins: new insights into membrane targeting of myristoylated and palmitoylated proteins. Biochim Biophys Acta 1999;1451:1–16. [PubMed: 10446384]

39. Resh MD. Membrane targeting of lipid modified signal transduction proteins. Subcell Biochem 2004;37:217–232. [PubMed: 15376622]

40. Burgoyne RD. The neuronal calcium-sensor proteins. Biochim Biophys Acta 2004;1742:59–68. [PubMed: 15590056]

41. O'Callaghan DW, Burgoyne RD. Role of myristoylation in the intracellular targeting of neuronal calcium sensor (NCS) proteins. Biochem Soc Trans 2003;31:963–965. [PubMed: 14505460]

42. O'Callaghan DW, Hasdemir B, Leighton M, Burgoyne RD. Residues within the myristoylation motif determine intracellular targeting of the neuronal Ca2+ sensor protein KChIP1 to post-ER transport vesicles and traffic of Kv4 K+ channels. J Cell Sci 2003;116:4833–4845. [PubMed: 14600268]

43. O'Callaghan DW, Haynes LP, Burgoyne RD. High-affinity interaction of the N-terminal myristoylation motif of the neuronal calcium sensor protein hippocalcin with phosphatidylinositol 4,5-bisphosphate. Biochem J 2005;391:231–238. [PubMed: 16053445]

44. O'Callaghan DW, Ivings L, Weiss JL, Ashby MC, Tepikin AV, Burgoyne RD. Differential use of myristoyl groups on neuronal calcium sensor proteins as a determinant of spatio-temporal aspects of Ca2+ signal transduction. J Biol Chem 2002;277:14227–14237. [PubMed: 11836243]

45. Streb JW, Miano JM. Cross-species sequence analysis reveals multiple charged residue-rich domains that regulate nuclear/cytoplasmic partitioning and membrane localization of a kinase anchoring protein 12 (SSeCKS/Gravin). J Biol Chem 2005;280:28007–28014. [PubMed: 15923193]

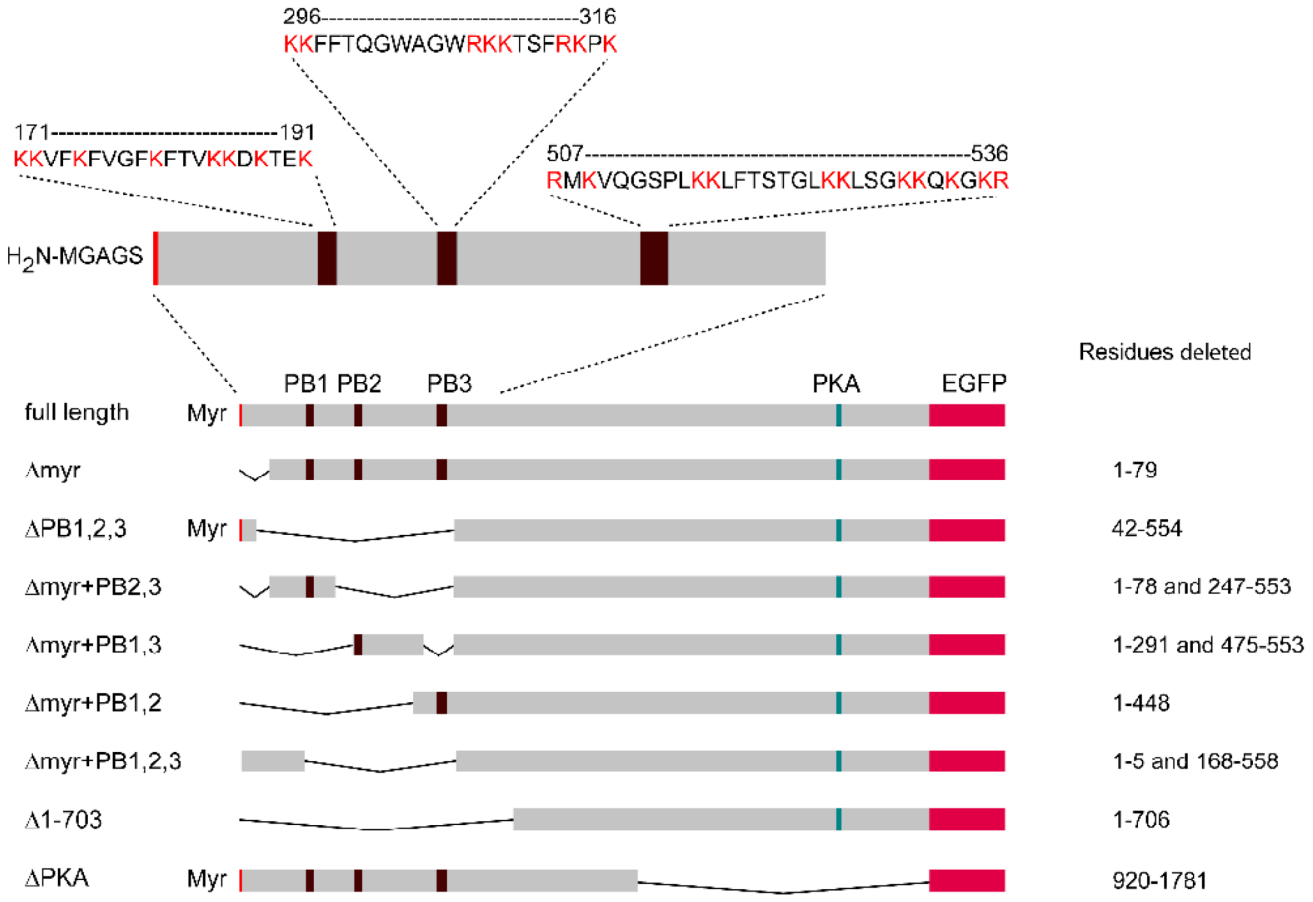

Figure 1.
Schematic diagram showing the position of the myristoylation site and the three polybasic regions (Myr, PB1, PB2 and PB3) in the full-length gravin and maps of the gravin-EGFP fusion protein constructs used in this study. The positions of deleted residues are also shown to the right of each construct.

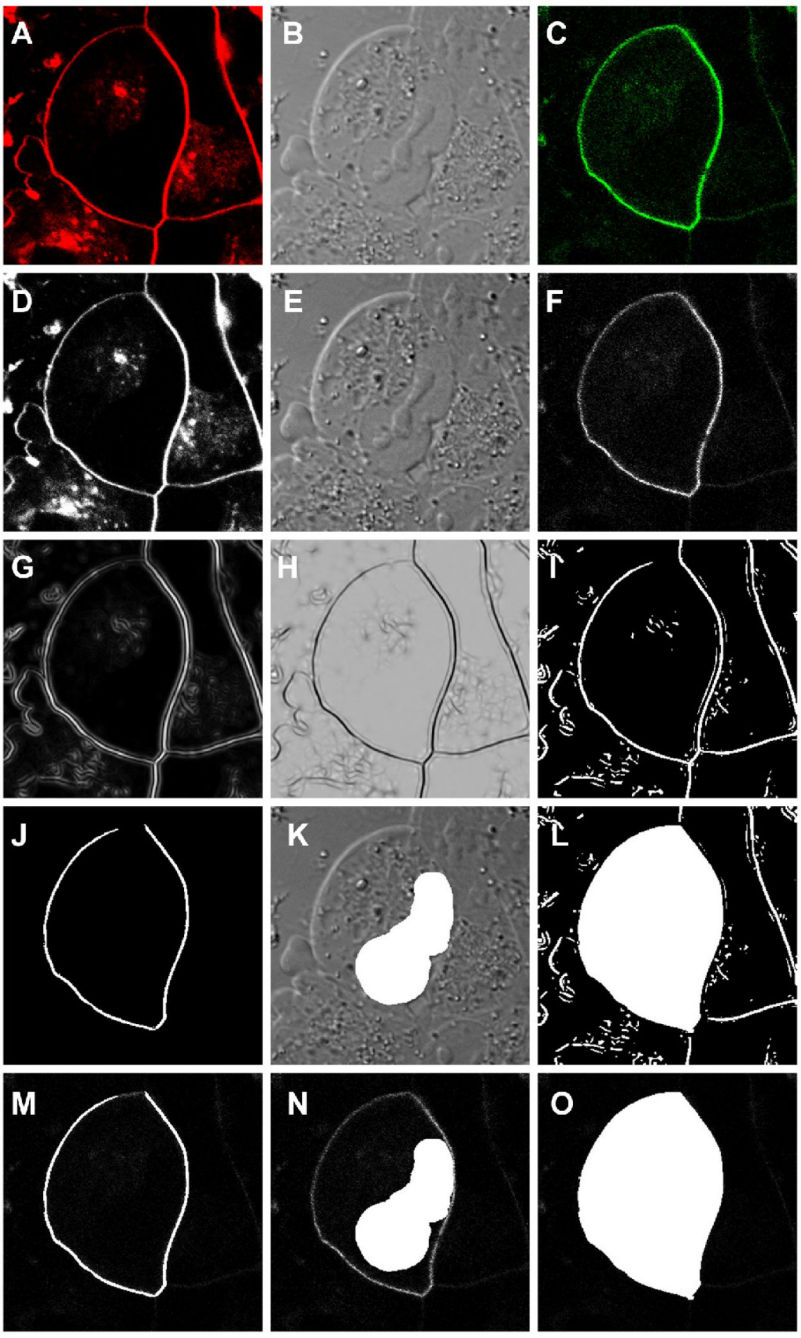

Figure 2.

A series of micrographs demonstrating the image processing steps used in the quantitative analysis of gravin distribution. A multi-channel confocal image captured at the level of the nucleus of a cell was split into the FM4-64 dye (red), the DIC and the gravin-EGFP (green) images (A, B and C respectively) and then converted to 8-bit grayscale images (D, E and F respectively) using Image J software. The 8-bit FM4-64 image was processed using a Hessian filter (Feature J plug-in) (G, H) and then the threshold of the resulting image was adjusted to highlight the plasma membrane region (I). This image was used to generate the region of interest for the membrane (J) and the entire cell (L). The nuclear ROI was defined by hand (K).

All three ROIs were then superimposed onto the 8-bit grayscale EGFP image (F) for fluorescence intensity measurements (M, N and O).

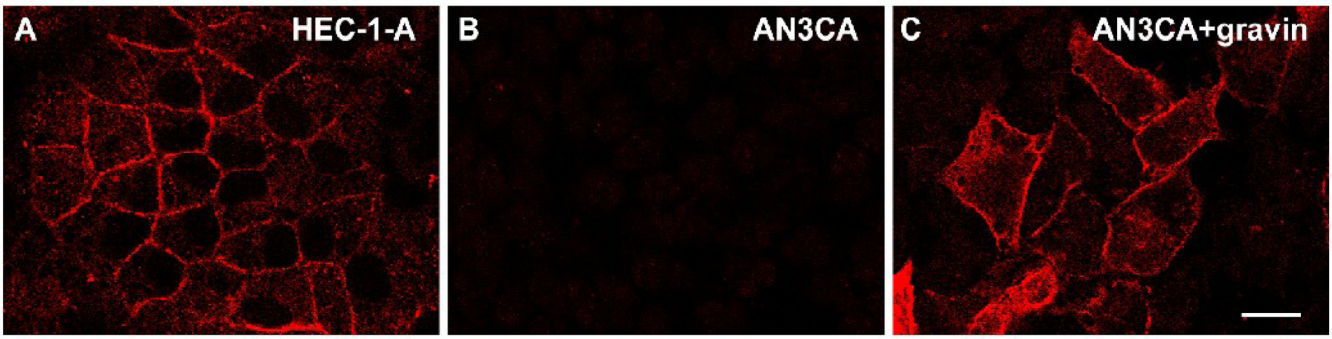

Figure 3.

Immunofluorescent images of gravin distribution in HEC-1-A and AN3 CA cells labelled with a monoclonal anti-gravin antibody. Endogenous gravin localized at the cell periphery in clusters of HEC-1-A cells (A). Endogenous gravin was not detected in AN3 CA cells using the same approach (B), but transiently expressed gravin was localized at the cell periphery in AN3 CA cells transfected with a full-length gravin construct (C). Scale bar, 20 μm.

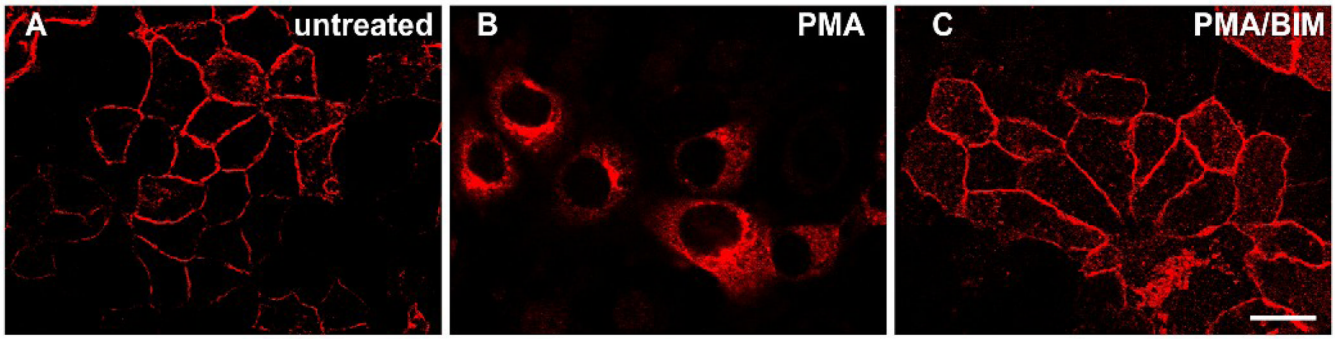

Figure 4.

Immunofluorescent images of HEC-1-A cells illustrating the effect of PMA treatment on gravin distribution. Gravin localized to the cell periphery in untreated cells (A), but underwent redistribution to a juxtanuclear regions after 30 minutes treatment with 200 nM phorbol 12-myristate 13 –acetate (B). Gravin distribution did not change in cells coincubated with 200 nM PMA and 1 μM bis-indolylmaleimide I (BIM) for 30 minutes (C). Scale bar, 20 μm.

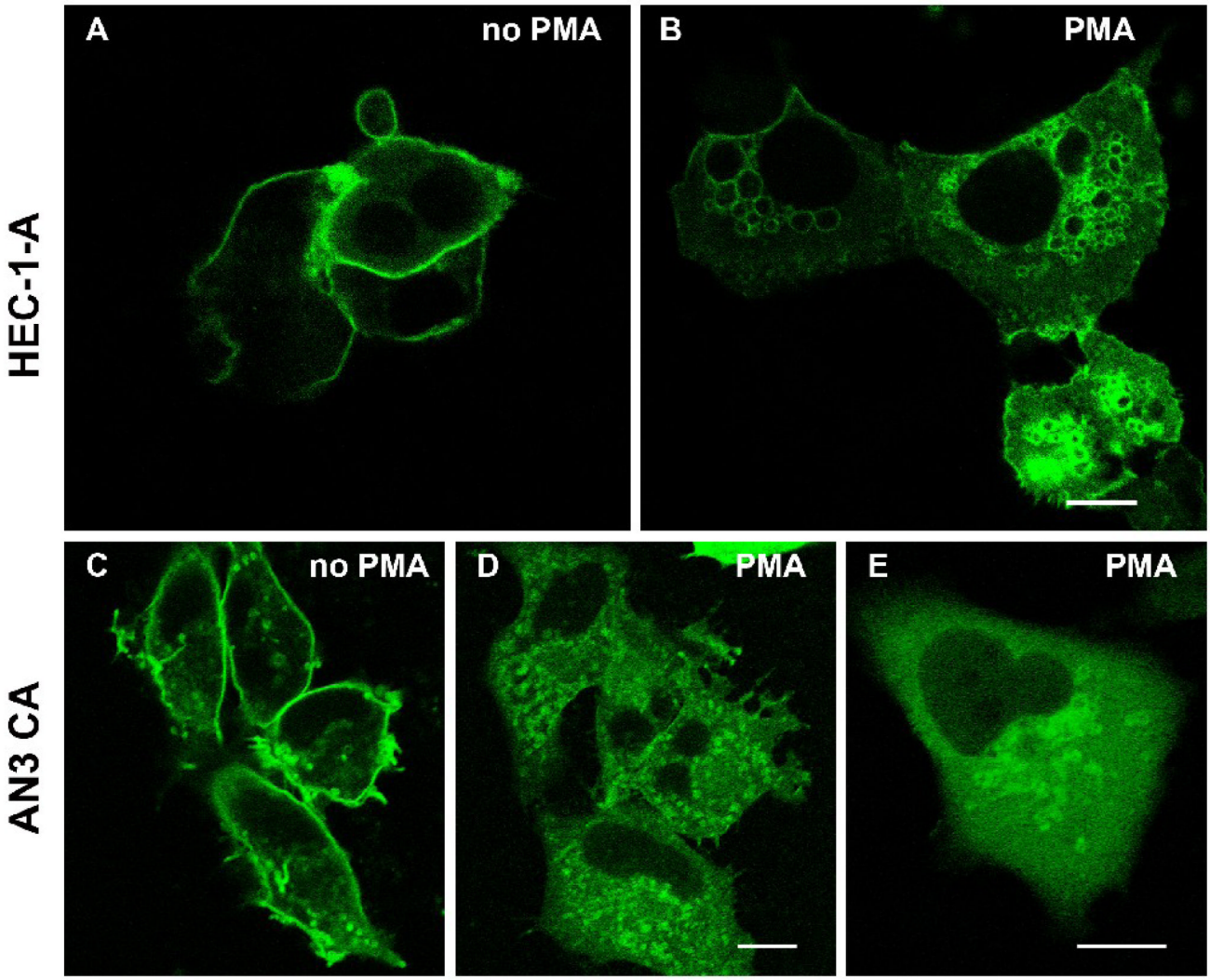

Figure 5.

Fluorescent images of HEC-1-A (A, B) and AN3 CA cells (C, D, E) transfected with a full-length gravin-EGFP construct. The gravin-EGFP fusion protein localized at the cell periphery in untreated cells (A, C), but translocated to juxtanuclear vesicles after PMA treatment (B, D, E). All scale bars, 10 μm.

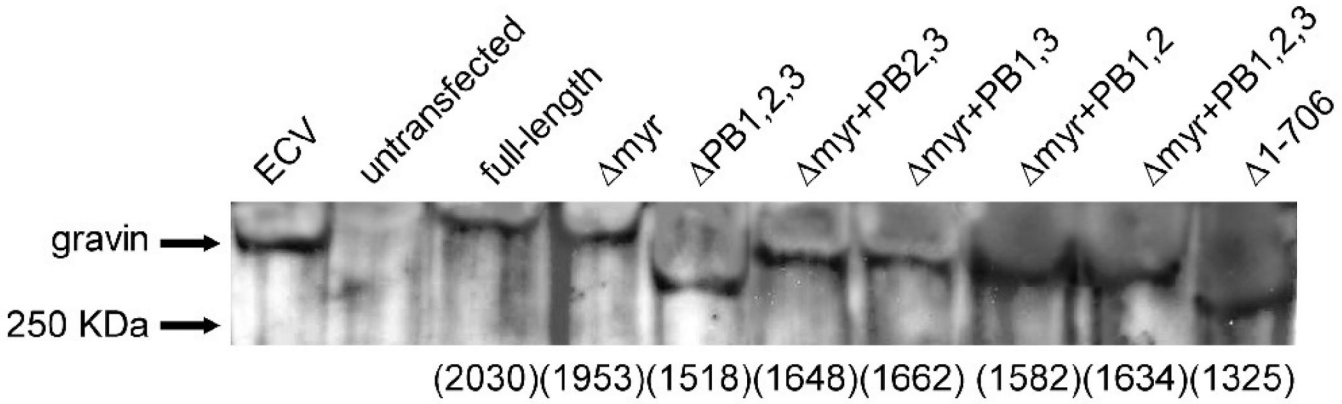

Figure 6.

A Western blot demonstrating the expression of full-length gravin-EGFP and its deletion mutants in AN3 CA cells. Sixty μg total protein was loaded in all lanes except the first lane, which was loaded with 10 μg of ECV304 cell lysate containing endogenous gravin (labeled gravin). The second lane was loaded with a lysate from untransfected AN3 CA cells. Other lanes were loaded with lysates from AN3 CA cells transfected with full-length and mutant gravin-EGFP constructs as labeled. The number of amino acids comprising each fusion protein is marked on the bottom of the blot.

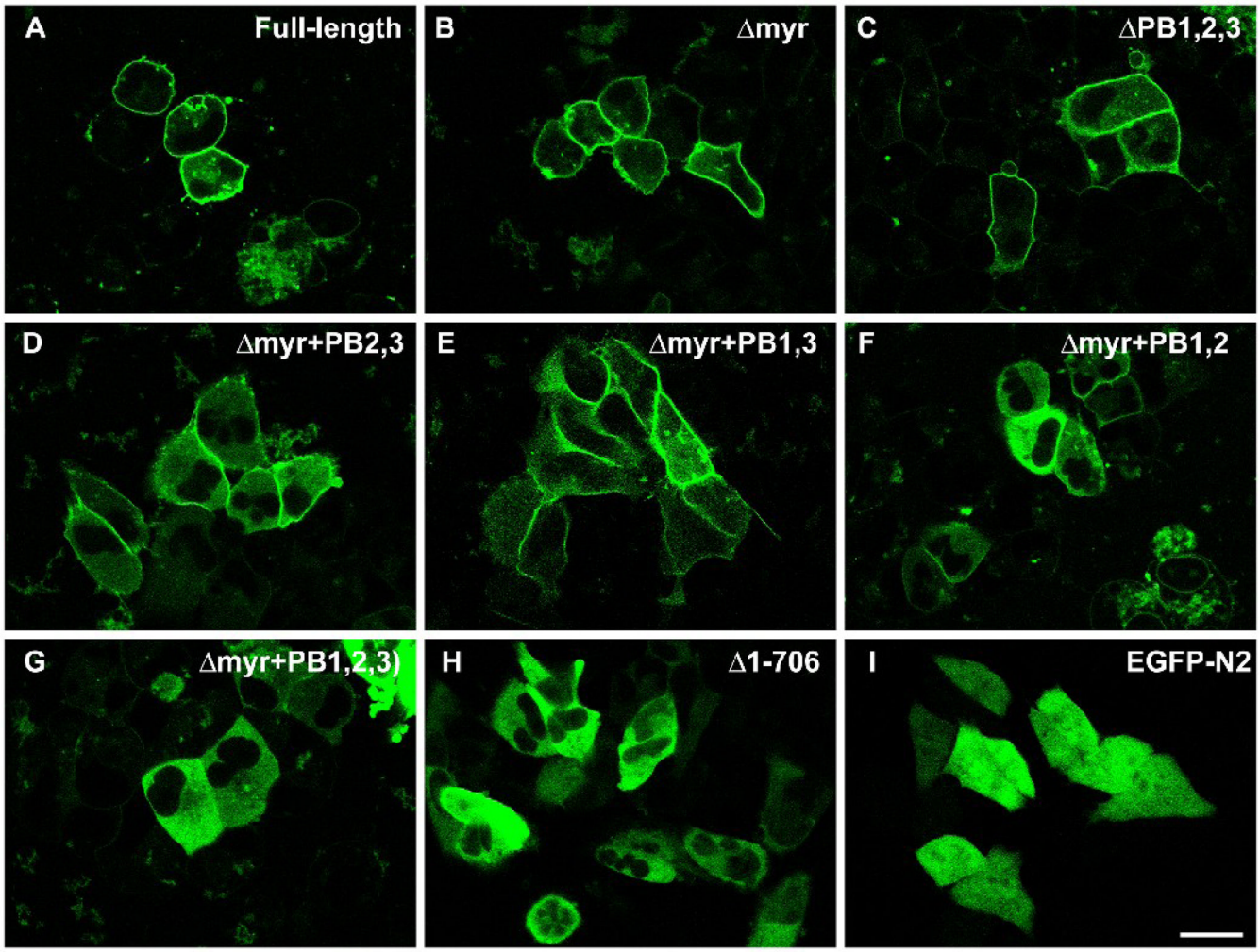

Figure 7.

Confocal images of AN3 CA cells expressing full-length gravin-EGFP (A), mutant gravin-EGFP constructs lacking different portions of the proposed membrane targeting domains as labeled (B–H), and EGFP-N2 alone (I). Deletion of the myristoylation site or all three polybasic regions did not significantly change the peripheral distribution of gravin-EGFP fusion protein (B, C). Mutant gravin-EGFP fusion proteins lacking the myristoylation site and different combinations of any two of the three polybasic regions lost the peripheral distribution to some degree (D–F). Deletion of the myristoylation site and all three polybasic region resulted in a construct that displayed a strictly cytosolic distribution similar to that displayed by EGFP-N2 except for the absence of nuclear labeling (G–I). Scale bar, 20 μm.

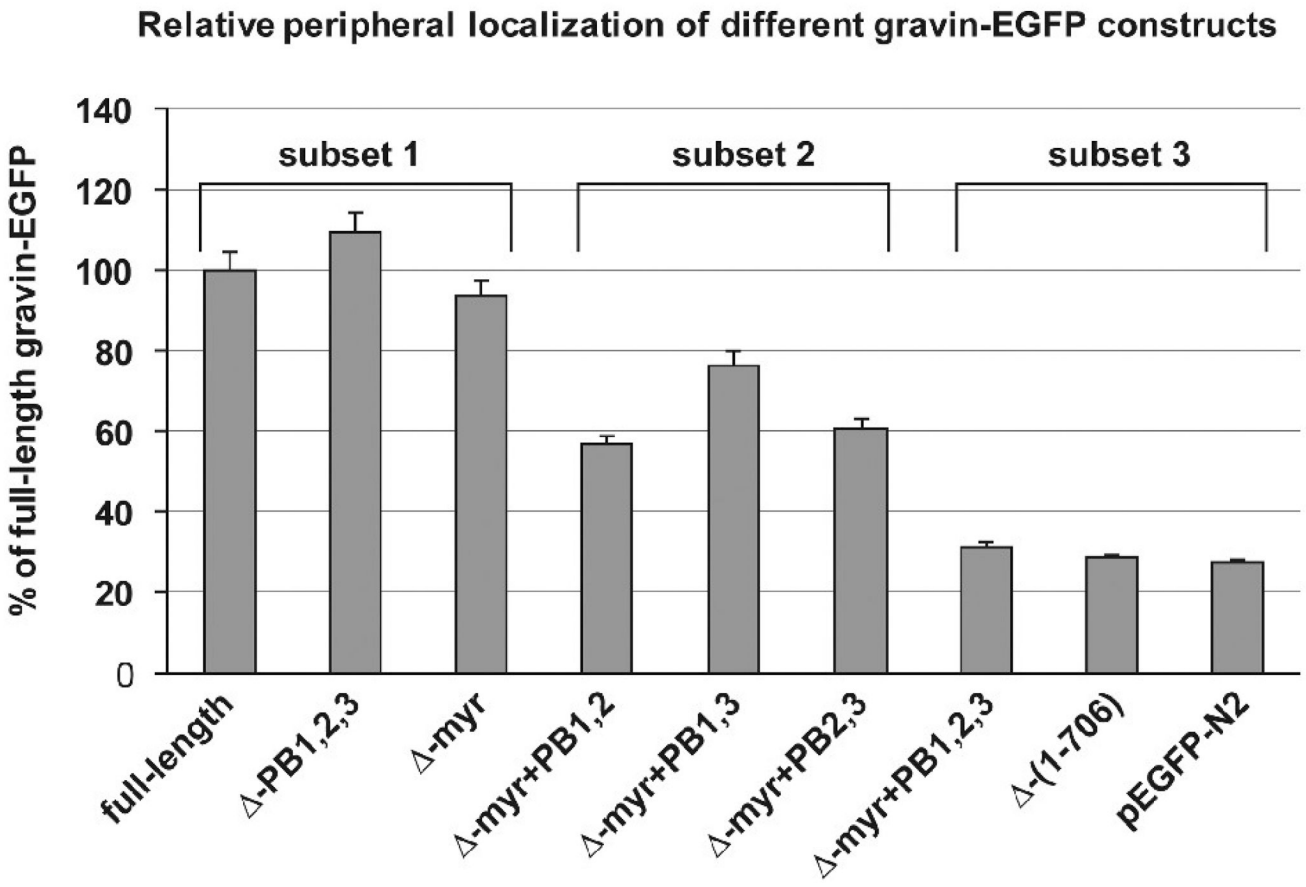

Figure 8.

A graph showing the relative EGFP fluorescence intensity at the cell periphery in cells transfected with the different gravin constructs. Values are plotted as a percentage of the relative peripheral fluorescence observed in cells expressing the full length gravin-EGFP construct. Statistical analysis (One way ANOVA followed by Scheffe post-hoc test) indicates that the samples fell into three statistically distinct subsets (subsets 1, 2, and 3) consisting of (1) full-length gravin, Δmyr gravin and ΔPB1,2,3 gravin, (2) gravin constructs lacking the myristoylation site and any two of the polybasic domains, and (3) gravin constructs lacking both the myristoylation site and all three polybasic domains or EGFP alone. Constructs in subsets 1 and 2 displayed significantly greater peripheral localization than the constructs in subset 3 ($p<0.01$). Error bars represent the standard deviation for each treatment set.

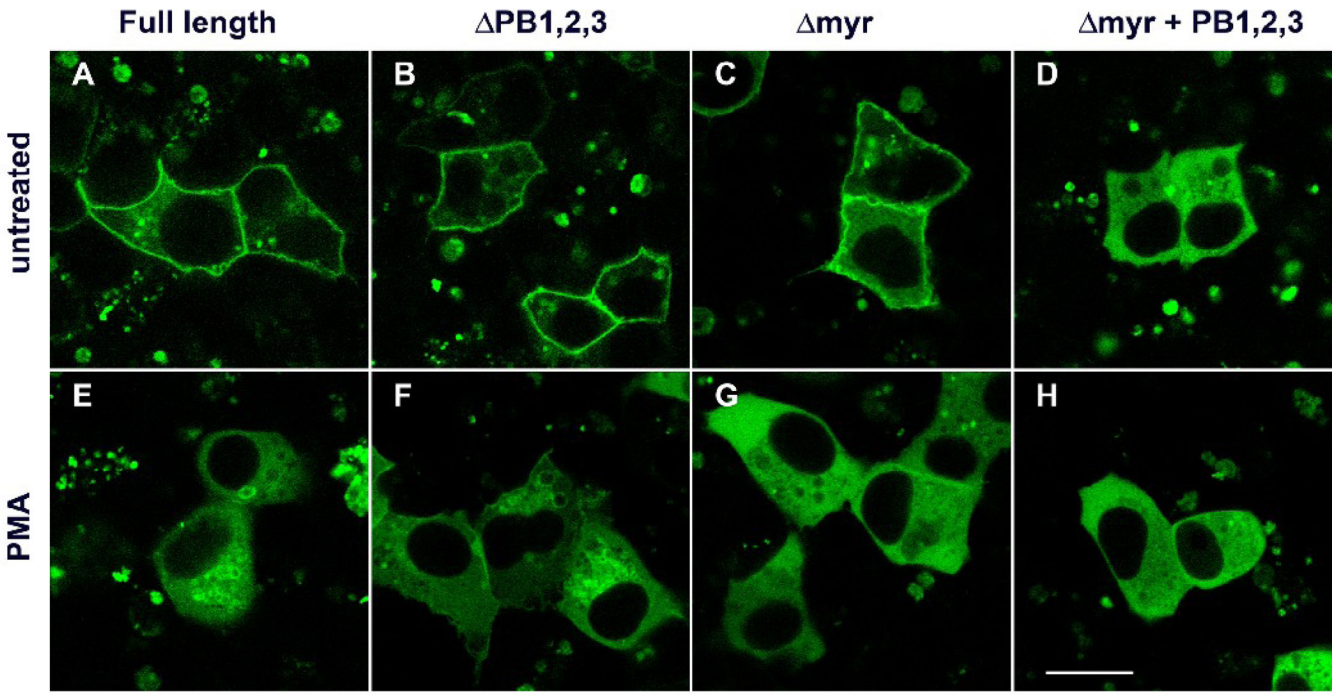

Figure 9.

Fluorescent images showing the role of membrane targeting domains in mediating PMA induced translocation of gravin-EGFP in HEC-1-A cells. Deletion of the polybasic regions (ΔPB1,2,3) did not affect targeting of gravin-EGFP to the juxtanuclear compartment after PMA treatment (B and F). However, deletion of the myristoylation site significantly altered translocation of gravin-EGFP in response to PMA and resulted in targeting of the construct to the cytosol only (C and G). PMA treatment had no effect on the cytosolic distribution of gravin-EGFP lacking the myristoylation site and all three polybasic regions (D and H). Scale bar, 20 μm.

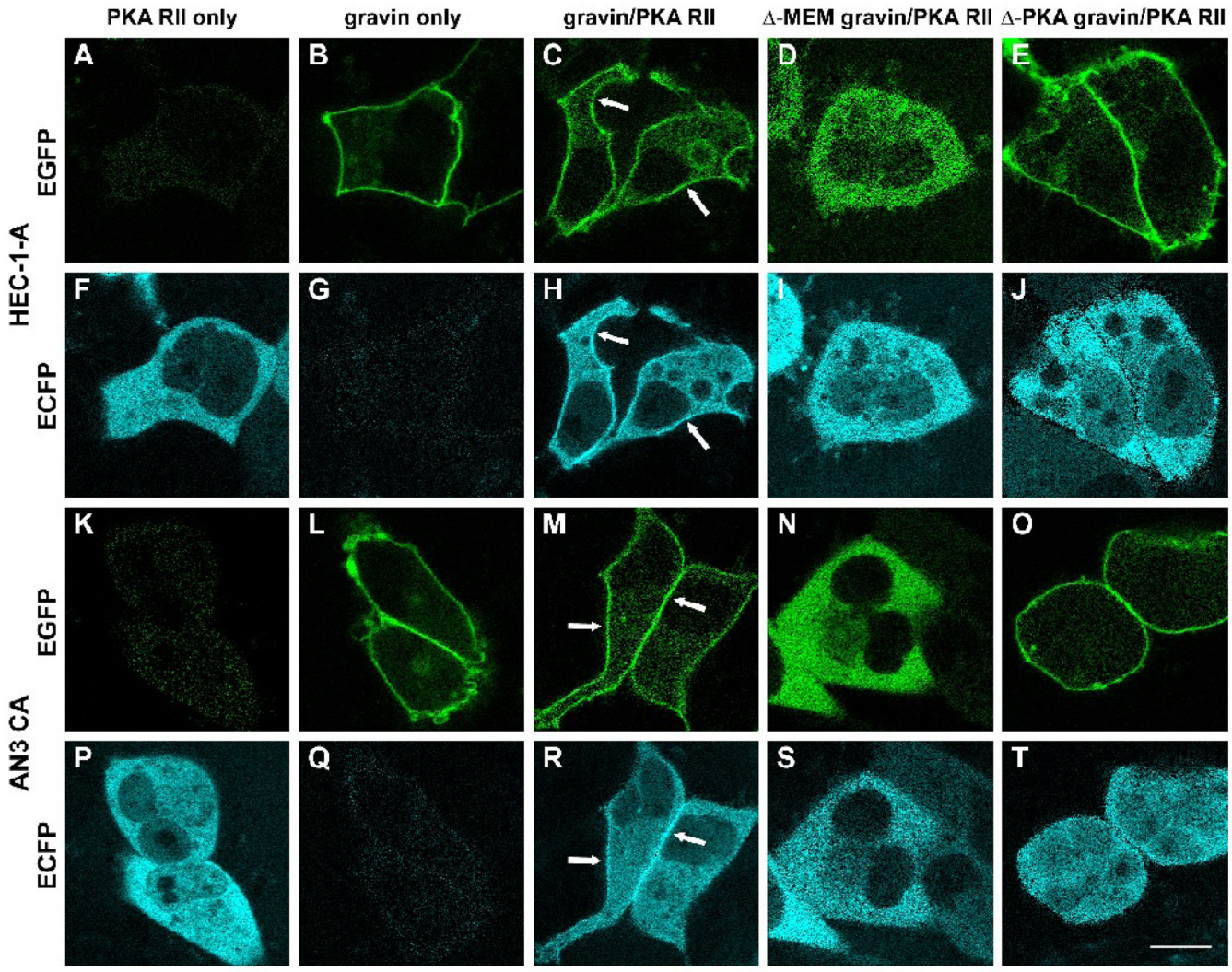

Figure 10.

Fluorescent images illustrating the effect of gravin on the subcellular distribution of PKA RII in HEC-1-A (A–J) and AN3 CA cells (K–T). In cells expressing PKA RII-ECFP alone, PKA RII-ECFP was distributed evenly throughout the cytosol and was not concentrated at the cell periphery (A,F, K, P). In contrast, PKA-RII-ECFP colocalized with gravin-EGFP at the cell periphery of cells co-expressing both PKA-RII-ECFP and gravin-EGFP (C,H, M, R)(arrows). That this apparent codistribution of EGFP and ECFP signals was not due to cross-over of the EGFP signal into the ECFP channel was confirmed by imaging cells expressing full length gravin-EGFP alone (B, G, L, Q). Localization of PKA RII ECFP at the cell periphery was dependent on the membrane targeting and the PKA binding domains being present in gravin. In cells co-expressing PKA RII-ECFP with either gravin-EGFP lacking the membrane binding domains (Δ-MEM gravin; D, I, N, S) or gravin-EGFP lacking the PKA binding domain (Δ-PKA gravin; E, J, O, T), PKA RII-ECFP distribution was diffuse in the cytosol and did not show concentrated localization at the cell periphery. Scale bar, 20 μm.

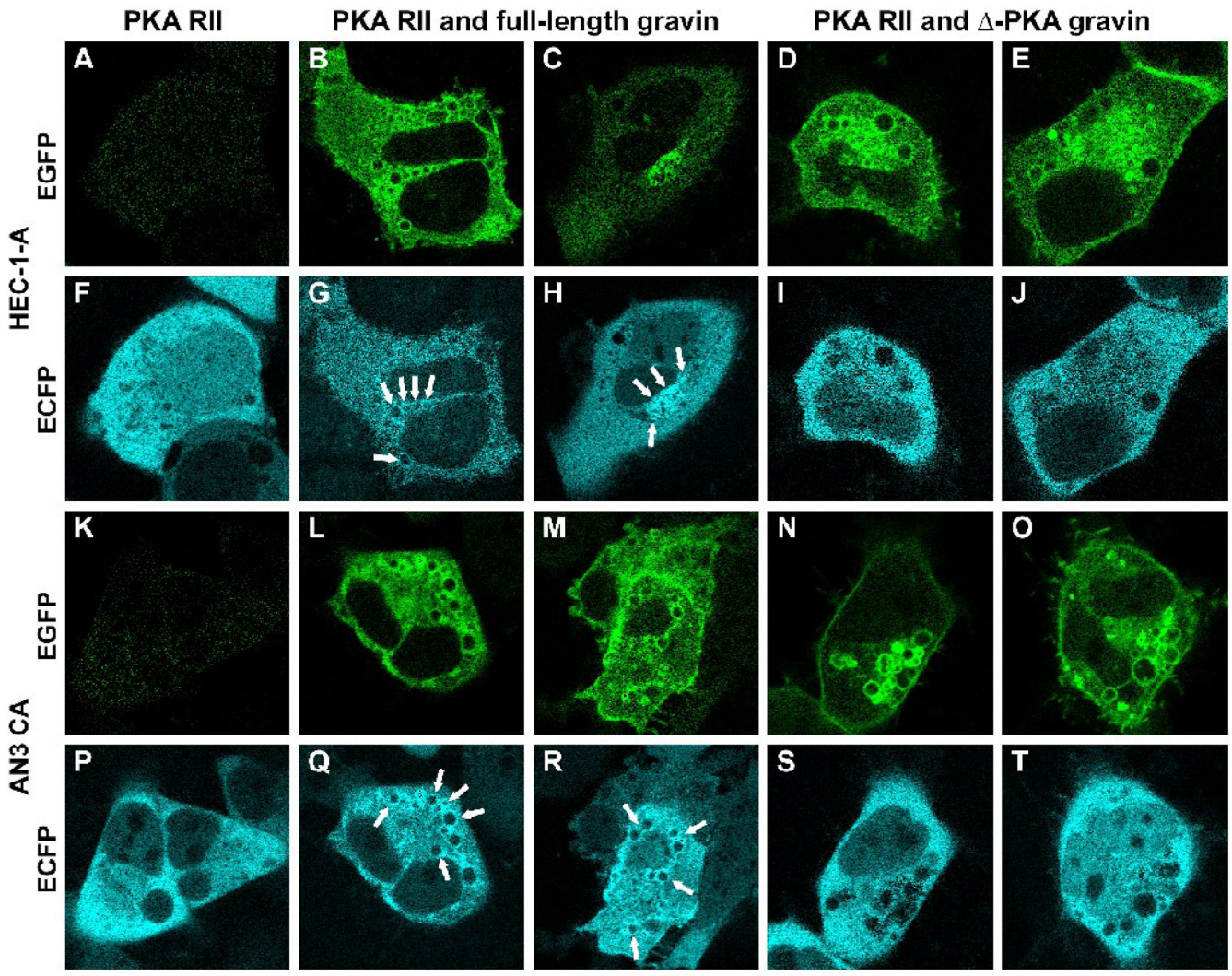

Figure 11.

Fluorescent images illustrating the effect of changes in gravin distribution on PKA RII distribution in HEC-1-A (A–J) and AN3 CA cells (K–T) after PMA treatment. PMA treatment did not affect PKA RII-ECFP distribution in cells expressing PKA RII-ECFP alone (A, F, K, P). Similarly, PKA RII-ECFP did not change distribution after PMA treatment in cells co-expressing PKA RII-ECFP and gravin-EGFP lacking the PKA RII binding domain (Δ-PKA gravin; D, I; E, J; N, S; O, T), although the gravin construct underwent redistribution to a vesicular compartment. In cells co-expressing full length gravin-EGFP and PKA RII-ECFP however, the gravin and PKA RII constructs both underwent redistribution from the cell periphery in response to PMA treatment and colocalized in the juxtanuclear region of the cells (B, G; C, H; L, Q; M, R). Arrows point to the vesicular membranes to where the PKA RII-ECFP redistributed. Scale bar, 20 μm.